Sensitivity analysis of the Rossi-Alpha Distribution and the early die-away time τ from the DDSI instrument due to modelling assumptions

Sophie Grape, Zsolt Elter, Erik Branger, Li Pöder Balkeståhl,

Division of Applied nuclear physics,
Department of Physics and Astronomy
Uppsala University, Sweden
E-mail: sophie.grape@physics.uu.se

Abstract

Under the Next Generation Safeguards Initiative, several different nuclear safeguards measurement techniques were studied. One of them was the Differential Die-Away Self-Interrogation technique, and the research showed that its early die-away time τ was proportional to the fuel assembly multiplication and thus sensitive to the fissile content of the fuel assembly under assay. A prototype instrument was later built and tested in the field, and the measurements showed that the instrument could be used successfully in the field.

This work builds on previous efforts, and systematically studies the effects of assumptions about the fuel properties (such as its dimensions) and its irradiation conditions in the reactor, on the Rossi-Alpha Distribution (RAD) and τ. The motivation is twofold, firstly to better understand if and what impacts such assumptions have on the RAD and τ, and secondly to investigate how well the simulation model used to estimate the RAD and τ is able to generalize to other fuel types and irradiation conditions than those modelled.

20 spent nuclear fuel assemblies currently residing in the Swedish interim storage for spent nuclear fuel were measured by the prototype DDSI instrument. The assemblies were modelled using Serpent2 and MCNP6 in this work. Fuel depletion calculations were performed assuming both a standard irradiation cycle and the actual irradiation history as provided by the operator. Fuel properties and irradiation conditions were also modified and their effect studied.

Based on the simulated DDSI instrument response in MCNP6, the RADs were created and τ determined. The analysis shows that each modelling assumption on its own affects both the RAD and the τ value. However, some of the individual effects work in opposite direction and cancel out when considered at the same time. For this reason, the default model is considered to be a good and valid approximation of the more complex one and results are expected to generalize well.

Keywords: Nuclear safeguards, DDSI, neutron coincidence, *tau (τ)*, modelling

1. Introduction

The DDSI instrument detects neutrons emitted from spent nuclear fuel. The detected neutrons originate from spontaneously fissioning radionuclides which act as a neutron source, interrogating the fissile content of the spent nuclear fuel. Depending on the nuclide inventory of the spent nuclear fuel, fission chains of various lengths develop and give rise to a distribution which describes the time evolution of the neutron population and is known as the Rossi-Alpha Distribution (RAD) [1]. That distribution is then used to determine the die-away time, τ, of the neutron population inside the nuclear fuel.

The DDSI technique was studied in detail under the Next Generation Safeguards Initiative, a project aiming to develop non-destructive assay instrumentation to verify operator declarations and fuel parameters, detect diversion of fuel material, estimate plutonium mass and decay heat, and to determine the reactivity of spent fuel assemblies [2]. Simulated responses were analysed to investigate the capability of the DDSI instrument to reach these goals (see for instance [3, 4]). A prototype DDSI instrument was also built and tested in the field, and it was shown that several algorithms developed to determine fuel assembly characteristics worked successfully on measured data [5,6].

The parameter τ is sensitive to the balance of fissile material and neutron absorbing isotopes, and has a high relevance in safeguards evaluations. The nuclide inventory of a spent nuclear fuel (and thus τ) depends on several things such as the fuel assembly's initial enrichment, burnup and cooling time. This work aims at investigating if and to what extent the RAD and τ are also affected by parameters which are often not (well)known to a nuclear inspector in the field, such as the fuel geometry, the irradiation history, and irradiation conditions. It does not aim at confirming previous results or predict safeguards-relevant properties.

Although results on the sensitivity of τ to modelling assumptions have not been published before, the sensitivity in calculated nuclide inventories due to approximations or uncertainties in the input (such as key design features and operating conditions) has been investigated extensively, see e.g. [7] and references therein. The power history has been found to be of minor importance for most actinides and fission products at the time of discharge, but the moderator temperature (and its density) has been identified as important in the physics calculations. The boron concentration has also been found to be important as it influences the neutron spectrum in the fuel. The impact of the fuel temperature is more difficult to assess as it is not measured directly, and it is associated with major uncertainties. Other works, such as [8], have also studied the effects of the UO_2 mass density, power levels and irradiation history on uranium and plutonium concentrations and found them to be of little importance. Actinide inventories, and particularly short-lived nuclides, were however found to be the most sensitive to irradiation history variations. Reference [9] reported on small effects on a number of calculated isotopic concentrations due to changes in fuel temperature, and [10] showed that for BWR burnup credit calculations, the control blade position is important because it affects the ^{239}Pu concentration in the fuel.

In safeguards assessments, it is rare to have access to detailed information about the fuels under assay and it may be necessary to make assumptions similar to those made in the simulations here. In the event that an inspector has access to detailed information about the fuel, an accurate model can be created, but at the expense that the model probably does not generalize well to fuels with other properties. In this work we investigate how systematic uncertainties from various modelling assumptions affect the RAD and the predictions of τ. We do this by studying the implications of various modelling assumptions on the Rossi-Alpha Distribution (RAD) and τ, for 20 spent nuclear fuel assemblies of Pressurized Water Reactor (PWR) type. The scope of this work does not cover investigations on if and how the modelling assumptions impact the DDSI capbility to detect diversion of fuel material, estimate plutonium mass, decay heat, or determine the reactivity of spent fuel assemblies.

2. The DDSI principle and instrument design

The DDSI technique is a passive non-destructive assay technique, relying on neutron coincidence counting, that has been developed to study nuclear material such as spent nuclear fuel. In such fuel, radionuclides such as ^{244}Cm undergo spontaneous fission and act as an internal neutron source that interrogates the fissile content of the fuel. Some of the neutrons emitted by e.g. ^{244}Cm thermalize in the water surrounding the fuel rods, and induce fissions in primarily ^{235}U, ^{239}Pu, and ^{241}Pu. Depending on the nuclide inventory of the spent nuclear fuel (and thus the fuel assembly multiplication), fission chains with various lengths will develop. This affects the possible detection of the correlated neutrons, and therefore of the RAD and its decrease over time as quantified by the early die-away time τ.

The value of τ can be determined from the RAD, which is a histogram describing the number of subsequent neutrons detected within a certain time window after the trigger neutron. The distribution can be described by a single exponential function in a limited time span, although the underlying physics can be explained by two different physical processes, each of which can be described by an exponential function. One process concerns neutrons coming from the same fission event, or from fast fission processes where the neutron has not thermalized before inducing fission. These neutrons typically have a fast die-away time (or a fast time component) which is determined mainly by the time needed for the neutron to reach the DDSI detectors and thermalize in the polyethylene around them (the die-away time of the detectors is approximately 19 μs). The second process concerns time-correlated neutrons coming from fission reactions in the same fission chain, where at least one second fission was induced by a thermal neutron. The second process may take much longer time than the first process, and its die-away time may extend up to hundreds of μs. The so-called early die-away time τ is a function of both processes and can be determined in a specific time range of the RAD, where properties of the spent nuclear fuel (such as abundance of fissile and neutron absorbing material) as well as properties of the DDSI instrument design, play a role. Reference [4] showed that in the time window of 4-52 μs, τ was found to be quadratically related to the SFA multiplication, which makes τ interesting in the context of spent nuclear fuel verification for nuclear safeguards purposes.

A model of the DDSI prototype instrument design is shown in Figure 1. There are four detector pods, symmetrically located around the FA. Each of them contains 14 ^{3}He-detectors, surrounded by polyethylene and encased in steel containers filled with air. Between the detector pods and the FA, there is a lead shield and a funnel which guides the fuel assembly into position, as it is inserted into the instrument from above.

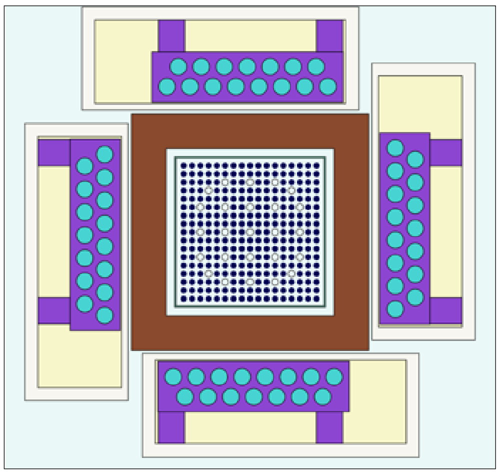

Figure 1. The DDSI instrument as implemented in MCNP. The fuel assembly is shown in the centre, surrounded by a lead shield (brown) and four detector pods. The ^{3}He detectors are shown in blue inside the pods, and the polyethylene surrounding them is shown in purple.

3. Modelling spent nuclear fuel and the DDSI instrument response

The 20 studied spent nuclear fuel assemblies are all PWR 17x17 fuel assemblies irradiated at the Ringhals nuclear plant in Sweden. They are produced by five different fuel manufacturers, but according to the fuel information in [11], 17 out of the 20 fuel assemblies are very similar with respect to fuel dimensions, while the remaining three have fuel rod dimensions which deviate from the other 17 fuel assemblies by less than 10%. The initial enrichment of all 20 fuel assemblies ranges between 2.1-3.9 %, the burnup ranges between 20-48 GWd/tU and the cooling times are approximately 10-35 years. The information provided to the authors at the time of this work does not include any information on whether or not there are Gd rods present in any of the fuel assemblies, and thus Gd rods were not modelled. Should additional information indicate that there are indeed such rods present, their impact would need to be studied using a different model since the burnup calculations in this work are made with a single-pin model, and thus assumes that all fuel rods are identical in the subsequent steps.

The Serpent2 code [12] was used to define a fuel pin model, deplete it and estimate its material composition. The fuel pin was placed in an infinite 2D lattice in Serpent2, and run in criticality source mode.

MCNP6 [13,14] was then used to construct a model of the DDSI instrument in water, sample spontaneous fission neutrons emitted by the spent nuclear fuel, transport the neutrons from the source to the DDSI instrument and estimate its response. A full fuel assembly was assumed, consisting of identical fuel rods where the material composition was taken from the output of the Serpent2 calculations. A spontaneous fission source was evenly distributed across all fuel pins, but restricted in the axial direction to 145 cm centred on the DDSI, because it was found that regions farther from the instrument do not contribute to the detector signal. It can be pointed out that the simulations do not include background contributions from e.g. (α, n)-reactions, which are randomly distributed in time and thus neutrons from such reactions do not contribute to the rate of time-correlated neutrons. The neutron detection was simulated with neutron coincidence capture tallies (F8 CAP in MCNP6) in the ^{3}He tubes. One hundred F8 tallies, each with 2 µs gates were used to make the RAD of true neutron coincidences. 5 million neutron histories were simulated, which was sufficient for most of the tallies to pass the ten statistical checks performed by MCNP6 (in a few tallies there were not enough hits to reliably estimate the slope of the probability density function). In order to determine τ, the RAD was created, showing the time difference between detected neutrons. A single exponential function was fitted to the RAD in the time window of 4-52 µs, as indicated in [4].

3.1 Modelling the fuel irradiation and DDSI instrument response

For the 20 studied fuel assemblies, two types of irradiation histories were considered in this work: a default irradiation and its actual irradiation. The default irradiation scheme was defined as 365 days of irradiation in the reactor, followed by 30 days of downtime. The reactor power was set so that a burnup of 10 GWd/tU per full cycle was achieved. The duration of the last cycle was adjusted to result in the desired discharge burnup value. The burnup step used was 0.5 GWd/tU. With respect to the actual irradiation scheme, this information was provided by the operator. It showed that the fuels had indeed undergone varying irradiation histories, ranging from some fuel assemblies having resided in the reactor only for two cycles, to others having been irradiated for up to five cycles. The burnup per cycle also varied both between fuel assemblies and between cycles. In the burnup calculations, the accurate irradiation histories as provided by the operator were used together with information on the average power level in each cycle, and 50-day burnup steps were used.

In order to systematically study the impact of also other changes than the fuel irradiation, the impact of the other parameters were studied in isolation. In Serpent2, the boron concentration in the water during irradiation was changed from 0 in the default case to 200 ppm, 630 ppm and 1100 ppm in three different simulations. The fuel temperature was 1500 K in the default case and 900 K in the realistic case; the fuel pellet density was 10.5 g/cm^3 in the default case and 10.41 g/cm^3 in the realistic case; the water density was 0.75 g/cm^3 in the default case and 0.723 g/cm^3 in the realistic case, and the fuel pellet radius was adjusted according to the values in [15]. With respect to the fuel pellet and fuel rod dimensions, either a default geometry representative of PWR fuel in general, or geometry and irradiation conditions based on the Westinghouse 17x17 Standard fuel in the Scale 6.1 manual [15], was used. Reference [11] conveys that dimensions for fuels from the other manufacturers are similar to those of Westinghouse 17x17 Standard fuel.

Also in MCNP6, changes were done to the model used to investigate the impact of the individual changes as well as their total effect. The effect of having guide tubes and a central instrumentation tube present (or not) was studied, and the fuel density and pellet radius were adjusted to match the values used in the corresponding Serpent2 calculations. In the final case, the total effect of all assumptions in both Serpent2 as well as MCNP6 was investigated.

The identified cases and details on model properties in Serpent2 and MCNP6 are shown in Table 1.

Modelling property	Software	Default properties	Realistic properties
1. Default irradiation history	Serpent2	Ideal irradiation history with 10 GWd/tU per 365-day irradiation cycle, followed by a 30-day outage.	-
2. Actual irradiation history	Serpent2	-	Actual irradiation history and power density as provided by the operator.
3. Boron concentration during irradiation	Serpent2	0 ppm	200 ppm 630 ppm 1100 ppm In case 9, 630 ppm was used.
4. UO_2 fuel temperature	Serpent2	1500 K	900 K
5. H20 density	Serpent2	0.75 g/cm^3	0.723 g/cm^3
6. Guide tubes and central instrumentation tube	MCNP6	No tubes	24 water-filled guide tubes and one central instrumentation tube
7. UO_2 fuel density	Serpent2/ MCNP6	10.50 g/cm^3	10.41 g/cm^3
8. UO_2 fuel dimension	Serpent2/ MCNP6	0.41 cm fuel pellet radius. 0.1 mm gap (void). Cladding outer radius equal to 0.48 mm. Pitch 1.26 cm.	0.4025 cm fuel pellet radius. 0.085 mm gap (void). Cladding outer radius equal to 0.475 mm. Pitch 1.26 cm.
9. All of the above assumptions	Serpent2/ MCNP6	All of the above default settings in Serpent and MCNP	All of the above realistic settings in Serpent2 and MCNP6.

Table 1. Default as well as more realistic properties used in the Serpent2 and MCNP6 modelling. The realistic values are taken from the Scale manual [15]).

4. Results

For three of the 20 fuel assemblies, representing fuels with both regular and irregular irradiation history, the impact of the modelling assumptions were studied in greater detail by implementing them one at a time to see their individual effects. These results can be found in section 4.1. For the remaining 17 fuel assemblies, three of the nine cases were investigated: the default case (case 1), the actual irradiation history (case 2) and when all assumptions are changed at once (case 9, denoted as “change all”). These results can be found in section 4.2.

4.1 Results from detailed investigations

This section presents separately the results on the RAD and τ from the studies of the three selected fuel assemblies.

4.1.1 Results on the RAD

Figure 2 shows the RADs and the fits to determine τ for the three fuel assemblies denoted fuel 1, 2 and 3.

One thing to immediately notice is the difference in RAD amplitudes between the fuels. The fuel with the highest RAD amplitude has an initial enrichment almost twice as large as of the other two fuel assemblies, but also a discharge burnup which is approximately twice as high. The fuel with the highest initial enrichment experienced an irradiation history similar to what was assumed in the default case, while the fuel with the lowest RAD amplitude experienced a very long first irradiation cycle and then a short period outside the reactor before being re-irradiated a second time. The authors acknowledge that this irradiation scheme seems out of the ordinary and could possibly be due to a reporting error by the operator; nevertheless, it is the information made available and it was therefore assumed to be true in this work. The fuel with a RAD amplitude between the other two fuel assemblies, experienced the same irradiation history as the fuel with the lowest RAD amplitude during the first two cycles and then resided outside the reactor for approximately ten years before being re-irradiated for two more cycles. Figure 2 also shows that the RAD for the default case (shown with black triangles) it is found roughly in the middle of all RADs, meaning that the various modelling assumptions separately result in both increased and decreased RAD amplitudes. However, for all three fuel assemblies:

- Increased boron content results in a higher RAD amplitude, as compared to the default case,

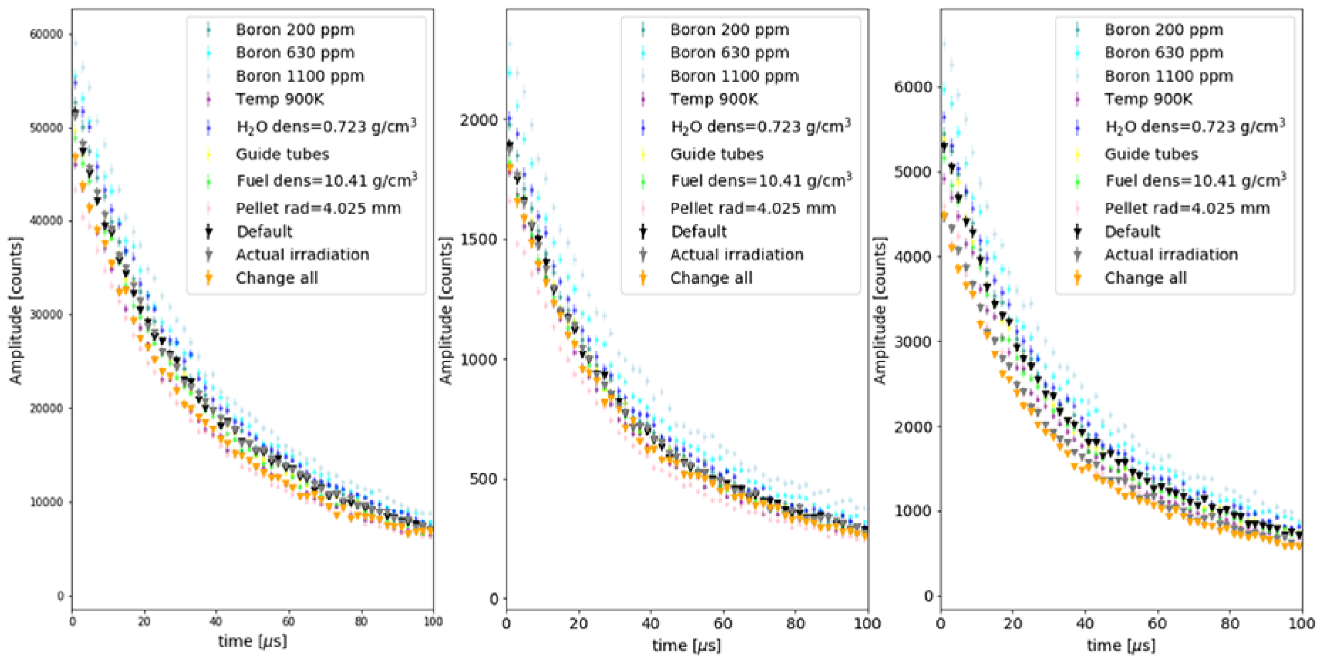

Figure 2. Resulting RAD distributions for the three fuel assemblies studied in greater detail: fuel 1 (left), fuel 2 (centre) and fuel 3 (right).

- Lower water density leads to a higher RAD amplitude, as compared to the default case,
- Decreasing the pin radius to more realistic values results in a lower RAD amplitude likely because this implies less material to assay, and
- Lowering the fuel temperature from 1500 K to 900 K changes the cross sections in the depletion calculations, which in turn results in a lower RAD amplitude.

The impact of the guide tubes is negligible, as is slightly lowering the UO_2 density to a more realistic value. The impact of the actual irradiation history is different in all three cases, probably because the default irradiation history is varying to different degrees from the actual irradiation history.

Interestingly enough, Figure 2 shows that for fuel 2, some of the modelling effects cancel out when all assumptions are changed simultaneously (case 9, change all). For fuel 1 and 3, case 9 results in a lower RAD amplitude (but not as pronounced as when changing only the fuel pellet radius, probably because the boron content offset partly compensates for this). For one of the fuels (fuel 3), the more realistic assumptions in the modelling, results in the lowest RAD amplitude of all cases (although it is close to changing only the irradiation history).

In order to better understand why the RAD changes in the way it does, the changes of eight selected nuclide concentrations, identified to be of most importance when determining τ, were studied in detail. The isotopes, as identified in [16], are $^{239\text{-}241}$Pu, ^{241}Am, ^{235}U, ^{238}U, ^{155}Gd and ^{149}Sm. In addition, we decided to include ^{242}Cm and ^{244}Cm because they contribute to both spontaneous fission and a constant background in a real measurement situation. Figure 3 shows how the selected nuclides vary for the different cases (not including the case where guide tubes are included in MCNP 6, since the depletion calculations in Serpent2 are the same as for the default case), for fuel 1. However, for all three fuel assemblies studied here, the concentrations change in practically the same way. One can note that the concentrations for several of the nuclides in Figure 3 change in very similar ways as the RADs in Figure 2.

In absolute terms, the nuclide concentrations change the most for ^{238}U, followed by ^{239}Pu and ^{235}U for all three fuel assemblies. In relative terms, there are variations among the three fuel assemblies, but large relative increases are typically seen for the fission products ^{149}Sm and ^{155}Gd and the two Cm-isotopes, ^{242}Cm in particular (especially for fuel 3). Figure 3 shows that the concentrations of ^{239}Pu, ^{241}Pu and ^{235}U grow with increasing boron concentration, and that a lower water density also leads to a higher concentration (both changes make the neutron spectrum harder). Making the fuel pellet radius smaller or lowering the fuel temperature, gives lower plutonium concentrations than in the default case. Changing the UO_2 density does not impact the plutonium concentration much, neither does the actual irradiation history except in the cases of the ^{242}Cm and ^{241}Pu concentrations for fuel 3 (the same fuel assembly for which the RAD amplitude changes as a function of irradiation history). The lowest ^{239}Pu and ^{241}Pu

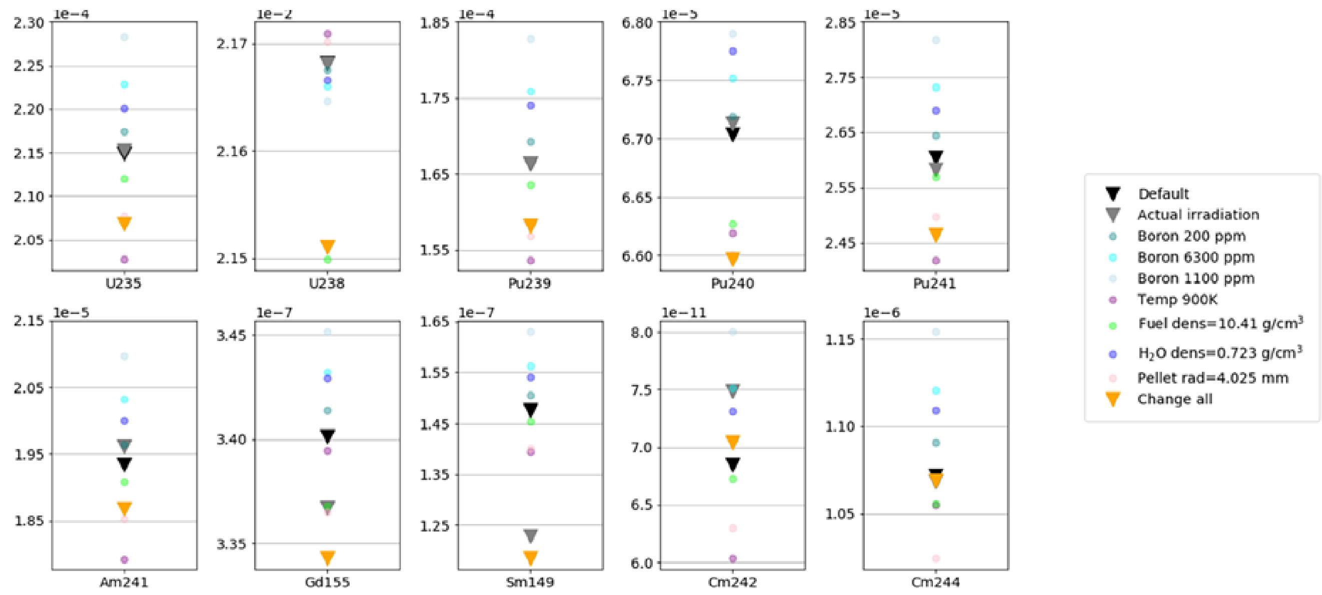

Figure 3: The subplots show how the selected nuclide concentrations (in units of 10^{24}/cm^3) vary for the different cases.

concentrations are found for a fuel temperature of 900 K and when all model assumptions are changed at the same time (case 9).

4.1.2 Results on τ

Values of τ for the simulated cases are shown in Table 2. They do not necessarily change in the same way as the RADs, since τ depends on the structure of the RAD. The values of τ for the fuel assembly with the highest initial enrichment (fuel 1) are consistently larger than for the two other fuel assemblies. It is not clear that increasing the boron content from 0 ppm (the default case), has an impact on τ. However, lowering the fuel temperature, the UO_2 density or making the fuel pellet radius smaller all seem to lower τ, although the magnitude of the effects are small in some cases. Lowering the water density has either a weak impact or no impact at all on τ. Making all changes at once, lowers τ in all three cases.

As seen in Table 2, modelling the actual irradiation history doesn't have a significant impact on τ, which remains the same when the uncertainties in the fits are taken into account, for all three fuel assemblies. The same holds true for changing the water density (even if this impacts the concentration of the three plutonium isotopes) or inserting guide tubes and an instrumentation tube. Increasing the boron content impacts τ, but differently for the different fuel assemblies. For fuel 1, a boron content of 200 ppm appears to considerably lower τ while increasing the boron content further restores τ to the same value as for no boron at all. For fuel 3, a boron content of 630 and 1100 ppm gives τ values, which are higher than for the default case. A lower fuel temperature gives a lower τ value for fuel 1, but not for the other two fuel assemblies. Lowering the fuel density lowers and decreasing the pellet radius lowers τ for fuel 1 and 3, but not for fuel 2.

4.2 Results for all fuel assemblies

For the remaining 17 fuel assemblies, three of the eleven assumptions were investigated: case 1, 2 and 9. For completeness, the results from the three fuels above can be found here as well.

4.2.1 Results on the RAD

The trend among the 17 spent nuclear fuel assemblies is that the irradiation history (case 2) has a low impact on the RAD amplitude. For the vast majority of the fuel assemblies, a visual inspection of the RAD data points reveal that these are the same within error bars, which show the uncertainty due to the number of simulated events in the Monte Carlo calculations, over the time interval 0-120 μs. In a few cases, the RADs do not completely overlap for times below 15 μs (fuels 19, 6 and 9), while the distributions sometimes overlap and sometimes not for another fuel (fuel 15). Only for one single fuel assembly (fuel 16), is the RAD associated with the actual irradiation history consistently lower than for the default irradiation. Inspecting the irradiation history for fuel 16 shows that it has undergone five irradiation cycles of rather varying length and cycle burnup, and resided outside the core for two years before being reinserted for a last irradiation cycle. For all fuel assemblies, the RAD amplitude for the most realistic case (case 9) is lower than, or approximately as large as, the RAD amplitude for the default case (case 1).

Cases investigated	Fuel 1		Fuel 2		Fuel 3	
	τ	Unc.	τ	Unc.	τ	Unc.
1. Default case	42.8	0.5	40.2	0.5	39.8	0.5
2. Actual irradiation	41.9	0.5	40.8	0.5	38.9	0.5
3.1. Boron concentration during irradiation = 200 ppm	41.3	0.4	40.8	0.5	39.7	0.5
3.2. Boron concentration during irradiation = 630 ppm	42.6	0.5	40.5	0.5	40.6	0.5
3.3. Boron concentration during irradiation = 1100 ppm	42.2	0.4	41.5	0.5	40.6	0.5
4. UO_2 fuel temperature = 900 K	40.8	0.5	39.7	0.5	38.6	0.5
5. H_2O density = 0.723 g/cm^3	42.3	0.5	40.6	0.5	39.8	0.5
6. Guide tubes and instrumentation tube present	41.9	0.5	41.0	0.5	38.9	0.5
7. UO_2 fuel density in Serpent and MCNP =10.41 g/cm^3	41.6	0.5	40.8	0.5	38.6	0.5
8. UO_2 fuel pellet radius in Serpent and MCNP=0.4025 cm	41.1	0.5	39.5	0.5	38.3	0.5
9. All of the above assumptions at once	40.9	0.4	39.6	0.5	37.6	0.4

Table 2. Determined τ values and the one sigma uncertainties in τ as determined by the fits, for the three selected fuel assemblies and the cases investigated in this work. All values are given in [μs].

4.2.2 Results on τ

With respect to the τ values, these are shown in Table 3 for all 20 fuel assemblies. One fuel assembly has a considerably higher τ than the other fuels; this fuel assembly has a relatively high initial enrichment and a medium discharge burnup after having been irradiated only two cycles. The fuel assembly with the lowest τ value is found to have a medium initial enrichment and a high burnup, having been irradiated for four cycles.

With respect to variations in τ with the modelling assumptions, the τ values for the default case (case 1) and the

Fuel	Default irradiation (case 1)		Actual irradiation (case 2)		Change all (case 9)	
	τ	Unc.	τ	Unc.	τ	Unc.
1	42.8	0.5	41.9	0.5	40.9	0.4
2	40.2	0.5	40.8	0.5	39.6	0.5
3	39.8	0.5	38.9	0.5	37.6	0.4
4	38.2	0.4	38.2	0.4	37.3	0.4
5	39.3	0.4	39.8	0.4	38.8	0.4
6	40.1	0.4	40.5	0.4	40.1	0.4
7	41.5	0.5	41.6	0.5	40.5	0.5
8	36.9	0.4	36.8	0.4	35.7	0.4
9	40.8	0.5	40.6	0.5	40.0	0.5
10	48.0	0.5	47.9	0.5	47.5	0.5
11	39.9	0.4	40.1	0.5	38.5	0.4
12	39.7	0.5	40.0	0.5	39.0	0.5
13	40.0	0.5	40.0	0.5	38.6	0.4
14	35.5	0.4	35.3	0.4	34.4	0.4
15	39.6	0.4	40.5	0.5	38.7	0.4
16	39.5	0.4	38.9	0.4	38.8	0.5
17	37.9	0.4	37.7	0.4	37.5	0.4
18	39.9	0.4	40.6	0.4	40.5	0.4
19	39.8	0.5	38.6	0.4	38.7	0.5
20	36.8	0.4	36.7	0.4	35.3	0.4

Table 3. The early die-away times τ and the one sigma uncertainties in τ as determined by the fit, for the 20 fuel assemblies and the three cases. All values are given in [μs].

seen that the RAD amplitude decreases for all fuel assemblies, and more so the higher the RAD amplitude is to start with. Among the nine fuel assemblies for which τ decreases the most (fuels 1, 3, 4, 7, 11, 13, 14, 15, 20), all but one fuel assemblies (fuel 1) have a fuel geometry consistent with that assumed in case 9. This indicates that using a more accurate fuel model leads to a lower τ value. The decrease in RAD amplitude seen for the 20 fuel assemblies in case 9 (as compared to case 1) is on average 2254 counts, and the decrease in τ is on average 0.92 µs.

For individual fuel assemblies, the largest change in τ between case 2 and case 1 (ie due to the irradiation history) is found for fuel 19, and it is 1.24 µs (or 3.12%). The largest change in τ between the case 9 and case 1 is found for fuel 3, and it is 2.22 µs (or 5.57%). The average change in τ between case 1 and 2 is 0.41 µs, and the average change in τ between case 1 and case 9 is 0.97 µs.

5. Summary and conclusion

The DDSI measurement technique offers a way to non-destructively assay the fissile material in spent nuclear fuel assemblies. It does so by quantifying the die-away time τ of the neutron population in a spent nuclear fuel assembly.

In this work, we have investigated how assumptions made in the modelling affect the resulting RADs and the τ values from the DDSI instrument. We have modelled a default irradiation history as well as the actual irradiation history, and we have made changes in the fuel geometry and the fuel irradiation conditions.

The results show that although each assumption in itself affects the RAD, most strikingly its amplitude, the τ values are less sensitive. The irradiation history, which can be both very difficult to obtain in practise and which for principal reasons should not be relied upon in safeguards evaluations, has very little or no impact on neither the RAD nor τ. However, lowering the fuel temperature, the fuel density or the pellet radius has an impact on both the RAD and τ. When making all changes simultaneously, the RAD amplitude is lowered for all fuel assemblies and τ is lowered for ten fuel assemblies (as compared to the default case). The largest change seen in τ between case 1 (the default case) and case 9 (change all) is 2.22 µs or 5.57%. The average change in τ is much lower, 0.97 µs. Based on these results, we consider the default model to be sufficiently good to estimate τ for different types of spent nuclear fuel assemblies with a 17x17 fuel geometry. However, considering that one of the objectives for developing the DDSI instrument was to estimate plutonium mass, we note that the modelling assumptions made in this work have a (varying) effect on the plutonium content of the spent nuclear fuel. The effect on the two fissile plutonium isotopes (^{239}Pu and ^{241}Pu) is larger than the resulting changes in τ. Although this may not be surprising, as τ captures the balance between fissile materials and neutron-absorbing materials and not the fissile material alone, it could be investigated in future work whether or not the simple model is suitable for estimating e.g. the plutonium mass or not.

Finally, we note that the depletion step in the model used for this work is based on a single-pin model, representative of all fuel rods in a fuel assembly. If there is information that indicates that this is not a valid assumption, such as the presence of Gd fuel rods in certain locations of the fuel assembly, a new model that does not assume that all fuel rods are identical needs to be developed to assess the impact of this on the RAD and τ.

6. Acknowledgement

The authors would like to thank the Swedish Radiation Safety Authority under contracts SSM2017-5979 and SSM2020-996, and express gratitude to our former colleague Klaes-Håkan Bejmer at Vattenfall for providing the fuel information.

7. References

[1] C. Kaplan, V. Henzl, H.O. Menlove, M.T. Swinhoe, A.P. Belian, M. Flaska, S.A.Pozzi, Utilizing simulated rossi-alpha distributions to develop new methods of characterizing spent nuclear fuel, in: PHYSOR Conference Proceedings, Kyoto, Japan, 2014

[2] S. Tobin, et al., “Experimental and Analytical Plans for the Nondestructive Assay System of the Swedish Encapsulation and Repository Facilities,” in IAEA Symposium, IAEA-CN-220-238, 2014.

[3] A. C. Trahan, Utilization of the Differential Die-Away Self-Interrogation Technique for Characterization and Verification of Spent Nuclear Fuel, Doctoral thesis, University of Michigan, 2016.

[4] A. C. Kaplan, V. Henzl, A. P. Belian, H. O. Menlove, M. T. Swinhoe, M. Flaska, S. A. Pozzi, “Determination of Spent Nuclear Fuel Assembly Multiplication with the Differential Die-Away Self-Interrogation Instrument,” Nuclear Instruments and Methods A, Vol. 757, No. 1, (2014).

[5] A. Trahan, G. E. McMath, P. Mendoza, H. Trellue, U. Backstrom, A. Sjoland, Preliminary Results from the Spent Nuclear Fuel Assembly Field Trials with the Differential Die-Away Self-Interrogation Instrument, 59th Annual Meeting of the Institute of Nuclear Materials Management (INMM 2018)

[6] A. Trahan et al., Results of the Swedish spent fuel measurement field trials with the Differential Die-Away Self-Interrogation Instrument, Nuclear Instruments and Methods in Physics Research Section A:

Accelerators, Spectrometers, Detectors and Associated Equipment, Volume 955, 1 March 2020, 163329, https://doi.org/10.1016/j.nima.2019.163329

[7] Nuclear Energy Agency, Spent Nuclear Fuel Assay Data for Isotopic Validation, State-of-the-art Report, NEA/NSC/WPNCS/DOC(2011), 5 June 2011

[8] G. E. Bosler, J. R. Phillips, W. B. Wilson, R. J. LaBauve and T. R. England, Production of Actinide Isotopes in Simulated PWR Fuel and Their Influence on Inherent Neutron Emission, LA--9343, DE82 021849, July 1982

[9] G. Radulescu I. C. Gauld G. Ilas, SCALE 5.1 Predictions of PWR Spent Nuclear Fuel Isotopic Compositions, ORNL/TM-2010/44, March 2010

[10] W. (B.J.) Marshall, B. J. Ade, S. Bowman, J. S. Martinez-Gonzalez , Axial Moderator Density Distributions, Control Blade Usage, and Axial Burnup Distributions for Extended BWR Burnup Credit, NUREG/CR-7224 ORNL/TM-2015/544

[11] Svensk Kärnbränslehantering AB, Spent nuclear fuel for disposal in the KBS-3 repository, Technical Report TR-10-13, https://skb.se/upload/publications/pdf/tr-10-13.pdf

[12] J. Leppänen et al., “The Serpent Monte Carlo code: Status, development and applications in 2013,” Annals of Nuclear Energy, 82, pp. 142-150 (2015).

[13] MCNP6 user’s manual version 1.0 edited by D. Pelowitz, LA-CP-13-00634 2013

[14] T. Goorley: Using MCNP5 for medical physics applications, LA-UR-05-2755

[15] Oak Ridge National Laboratory, Scale: A Comprehensive Modeling and Simulation Suite for Nuclear Safety Analysis and Design, ORNL/TM-2005/39 Version 6.1, June 2011

[16] L. Caldeira Balkeståhl, Zs. Elter, S. Grape, Parametrization of the differential die-away self-interrogation early die-away time for PWR spent fuel assemblies, ESARDA BULLETIN, No. 58, June 2019